

# Sr<sub>2</sub>BN<sub>2</sub>I: A Strontium Iodide Compound with Isolated BN<sub>2</sub><sup>3-</sup> Units

Franziska E. Rohrer and Reinhard Nesper

*Inorganic Chemistry Laboratory, Eidgenössische Technische Hochschule Zürich, Universitätsstrasse 6, CH-8092 Zürich, Switzerland*

Received April 13, 1998; in revised form September 11, 1998; accepted September 11, 1998

The compound Sr<sub>2</sub>BN<sub>2</sub>I was synthesized from a mixture of the binary components Sr<sub>3</sub>N<sub>2</sub>, SrI<sub>2</sub>, and BN in sealed steel ampoules at 1150 K. The structure was refined from single crystal data. Sr<sub>2</sub>BN<sub>2</sub>I crystallizes with the monoclinic symmetry *P*2<sub>1</sub>/*m* (No. 11) with *a* = 10.284(7) Å, *b* = 4.224(3) Å, *c* = 13.246(9) Å, β = 90.87(6)°, *Z* = 4, and *V* = 575.3(7) Å<sup>3</sup>. The structure is built from isolated BN<sub>2</sub><sup>3-</sup> anions and quite distorted Sr<sub>6</sub>I octahedra. © 1999 Academic Press

## INTRODUCTION

Since the work of Goubeau and Anselmet [1] in 1961, the linear nitrido borate anion BN<sub>2</sub><sup>3-</sup>, which is isoelectronic to CO<sub>2</sub>, has been known [1]. Some interest focused on nitrido borate compounds because some of them can catalyze the phase transition from hexagonal to cubic boron nitride [2]. Pyykkö performed general calculations on linear three-atomic molecules and ions with 16 valence electrons comparing relative energies and vibration spectra [3]. Close to 20 new pure nitrido borate compounds and a few nitrido carbido borates forming double salts with chlorine, bromine, and oxygen have been reported over the recent decade [4, 5]. Recently, we reported on four new halogenide double salts, M<sub>2</sub>BN<sub>2</sub>X, with *M* = Ca, Sr and *X* = F, Cl [6] containing nitrido borate anions. We report here on the new compound Sr<sub>2</sub>BN<sub>2</sub>I, which was synthesized during systematic explorations of nitrido borate halogenide mixed crystal systems.

## EXPERIMENTAL

The compound is synthesized from stoichiometric amounts of strontium nitride, Sr<sub>3</sub>N<sub>2</sub>, strontium iodide, SrI<sub>2</sub>, and boron nitride. The precursors were well mixed and heated to 800 K in a stainless steel ampoule for 25 h. The temperature was then increased by 50 K/h to 1150 K, lowered to 1020 K by 1 K/h, and kept there for 50 h. The product is a light yellow powder. Single crystals are thin, transparent platelets. Observed and calculated powder patterns are given in Fig. 1, which shows that the main product

is Sr<sub>3</sub>N<sub>2</sub>. Two visible impurity peaks at about 2θ 29° and 49° can be assigned to SrO. The compound is sensitive to air and moisture, and decomposes in contact with air quite readily. The crystal structure was determined by single crystal X-ray diffraction. Table 1 contains the crystal data and the results of the X-ray measurement. The systematic absences belong to the space group *P*2<sub>1</sub>/*m* (No. 11). The structure was solved by direct methods and refined by the full-matrix least-squares procedure [7]. The residual difference electron density did not give indications for further atoms, for split positions, or for statistical occupations. Atomic coordinates and displacement parameters are listed in Table 2. Structure factor tables and further information may be obtained upon request.<sup>1</sup>

## CRYSTAL STRUCTURE AND DISCUSSION

Sr<sub>2</sub>BN<sub>2</sub>I belongs to a series of isostochiometric compounds M<sub>2</sub><sup>+</sup>BN<sub>2</sub>X (X = Hal) which despite their close chemical relation differ considerably in their crystal structures. Despite the fact that most nitrido borate fluorides and chlorides of different metals are isotypic for one and the same halogenide species, the change of the halogenide anion type induces a structural change in all cases investigated so far. In this respect, it is not surprising that Sr<sub>2</sub>BN<sub>2</sub>I forms a structure type which is characterized by slightly puckered layers of edge-sharing [Sr<sub>2/2</sub>Sr<sub>4/4</sub>I]<sup>3+</sup> octahedra which are moderately distorted (346 pm ≤ *d*(Sr–I) ≤ 363 pm). The structure is displayed in Fig. 2. The [Sr<sub>2</sub>I]<sup>3+</sup> layers are separated by groups of BN<sub>2</sub><sup>3-</sup> anions which are either perpendicular or parallel to the layers giving rise to the puckering. The structural motif shows quite nicely the mutual space requirements of the different components of the structure. Clearly, the larger iodine ions give rise to the relatively large condensation of the [Sr<sub>2</sub>I]<sup>3+</sup> substructure, which is due to the higher coordination number of the I<sup>-</sup> anions. In the series of the M<sub>2</sub>BN<sub>2</sub>X compounds the coordination numbers are 4 for F<sup>-</sup> in CaBN<sub>2</sub>F and Sr<sub>2</sub>BN<sub>2</sub>F [5],

<sup>1</sup>Two pages of supplementary data are available directly from the authors.

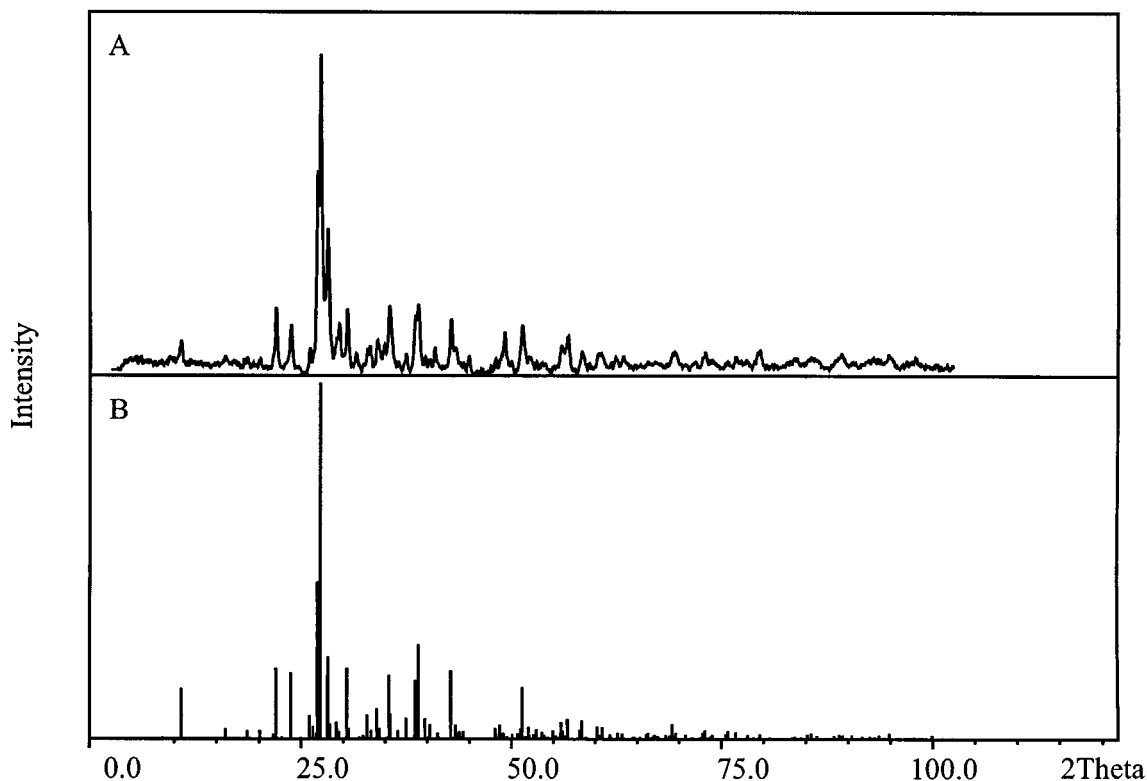


FIG. 1. X-ray powder diagrams of  $\text{Sr}_2\text{BN}_2\text{I}$ : (A) observed powder diagram of  $\text{Sr}_2\text{BN}_2\text{I}$ ; (B) calculated powder diagram of  $\text{Sr}_2\text{BN}_2\text{I}$ .

5 for  $\text{Cl}^-$  in  $\text{CaBN}_2\text{Cl}$  and  $\text{Sr}_2\text{BN}_2\text{Cl}$  [5], 5 and 6 for  $\text{Cl}^-$  in  $\text{EuBN}_2\text{Cl}$  [5], and 6 for  $\text{I}^-$  in  $\text{SrBN}_2\text{I}$  [5], but only 4 for  $\text{Br}^-$  in  $\text{BaBN}_2\text{Br}$  [5]. Obviously, the larger  $\text{Ba}^{2+}$  cations change the size ratios. This becomes quite obvious on comparison of the structures of fluorides, the isostochiometric chlorides, and the iodide in Fig. 3. In all cases observed so far, there is a clear separation between the halogenide and the nitrido borate substructures. On the one hand, this is due to the different strength of the coulomb interactions, being much stronger for the  $M-X$  contacts. This can be seen by simple lattice energy calculations using formal point charge distributions and the Ewald summation method [9]. As there is a close correspondence of the formal charges of the different anions according to  $X^-$  and  $(\text{N} = \text{B} = \text{N})^{3-}$  or  $\text{N}^- = \text{B}^- = \text{N}^-$ —e.g., all anions may be considered to carry unit charges—there seems to be not too much bias by introduction of the chosen formal charges. In other words, one could simplify the electrostatic situation by writing  $(\text{Sr}_2)^{4+}(\text{Y}^-)_3\text{X}^-$ , which at first glance does not give rise to any obvious preference for specific interactions. The comparison of  $M-N$  and  $M-X$  distances clearly reveals that the former are always the shorter. Considering this situation it becomes even more clear that the  $M-X$  contacts are energetically dominant, because the point potentials of all halogenide sites are, despite the type of

the halogenide, larger by a factor of about 2 than those of the nitrogen positions. We assume that this difference is the main reason for the segregation into different substructures.

However, the actual form of the  $[\text{M}_2\text{X}]^{3+}$  substructures seems to be controlled by the shape of the nitrido borate anions and by the relative anion and cation sizes. In the case of the fluorides  $[\text{M}_2\text{BN}_2\text{F}]^{3+}$  ( $M = \text{Ca}, \text{Sr}$ ), one-dimensional double chains of edge-sharing tetrahedra form the  $\text{M}_2\text{F}$  substructure while the  $\text{BN}_2^{3-}$  units surround these strands (cf. Fig. 3a). Not very much different is the arrangement for the chlorides  $[\text{M}_2\text{BN}_2\text{Cl}]^{3+}$  ( $M = \text{Ca}, \text{Sr}$ ), but the  $[\text{M}_2\text{Cl}]^{3+}$  substructure consists of double chains of edge-sharing quadratic pyramids (cf. Fig. 3b) which again are completely surrounded by  $\text{BN}_2^{3-}$  anions [5, 6]. The same general arrangement is still found in  $\text{Eu}_2\text{BN}_2\text{Cl}$ , but the  $[\text{Eu}_2\text{Cl}]^{3+}$  part is now set up by octahedra and quadratic prisms  $[\text{Eu}_{2/2}\text{Eu}_{3/3}\text{Cl}]^{3+} + [\text{Eu}_{6/3}\text{Cl}]^{3+}$  forming a triple polyhedral strand (Fig. 3c, [5]). Obviously, the somewhat larger  $\text{Sr}_6\text{I}$  groups in  $\text{Sr}_2\text{BN}_2\text{I}$  cannot be enveloped by the  $\text{BN}_2^{3-}$  units from all sides and thus instead of one-dimensional strands a layer structure arises (cf. Fig. 2). All the  $[\text{M}_2\text{X}]^{3+}$  partial structures are interpreted as polymeric complex cations in which the  $X$  atoms form the centers of the complexes. This view is supported by related complexes in quite

**TABLE 1**  
Crystallographic Data for Sr<sub>2</sub>BN<sub>2</sub>I

Formula	Sr <sub>2</sub> BN <sub>2</sub> I
Molecular weight [g/mol]	340.97
Space group	<i>P</i> 2 <sub>1</sub> / <i>m</i> (No. 11)
Volume [Å <sup>3</sup> ]	575.3(7)
Lattice constants	<i>a</i> = 10.284(7) Å <i>b</i> = 4.224(3) Å <i>c</i> = 13.246(9) Å <i>β</i> = 90.87(6)°
Formula units	4
Density g/cm <sup>3</sup>	3.936
Absorption coef. μ [mm <sup>-1</sup> ]	23.758
Crystal size [mm]	0.2 × 0.1 × 0.06
Data collection	Siemens SMART PLATFORM with CCD Detector Graphite monochromator
Measuring method	ω-scan
2θ <sub>max</sub>	72.66
Measured reflections	10776
Unique reflections	3060, <i>R</i> <sub>int.</sub> = 0.071
Solution	direct methods
Refinement method	SHELXL96
Parameters, restrictions	61, 0
<i>R</i> -value [ <i>I</i> > 2σ( <i>I</i> )]	<i>R</i> <sub>1</sub> = 0.039, <sup>a</sup> <i>wR</i> <sub>2</sub> = 0.077 <sup>b,c</sup>
<i>R</i> -value for all data	<i>R</i> <sub>1</sub> = 0.068 <sup>a</sup> , <i>wR</i> <sub>2</sub> = 0.085 <sup>b,c</sup>
maximal and minimal <i>e</i> <sup>-</sup> /Å <sup>3</sup>	1.691 and -2.16
Extinction coefficient	0.0078(4)

Note.  $\text{Goof} = \sqrt{\frac{\sum(w(F_o^2 - F_c^2)^2)}{(n-p)}}$ ;  $R_{\text{int}} = \frac{\sum(F_o^2 - \bar{F}_o^2)}{\sum F_o^2}$ ; *n* = no. of reflections, *p* = no. of parameters.

$${}^aR_1 = \frac{\sum(F_o - F_c)}{\sum F_o}$$

$${}^b\text{w}R_2 = \sqrt{\frac{\sum(w(F_o^2 - F_c^2)^2)}{\sum w(F_o^2)^2}}$$

${}^c\text{w} = \frac{1}{\sigma^2(F_o^2) + (g \cdot P)^2 + k \cdot P}$ ;  $P = \frac{\text{Max}(F_o^2, 0) + 2 \cdot F_c^2}{3}$ ; *k*, *g* = weighting factors.

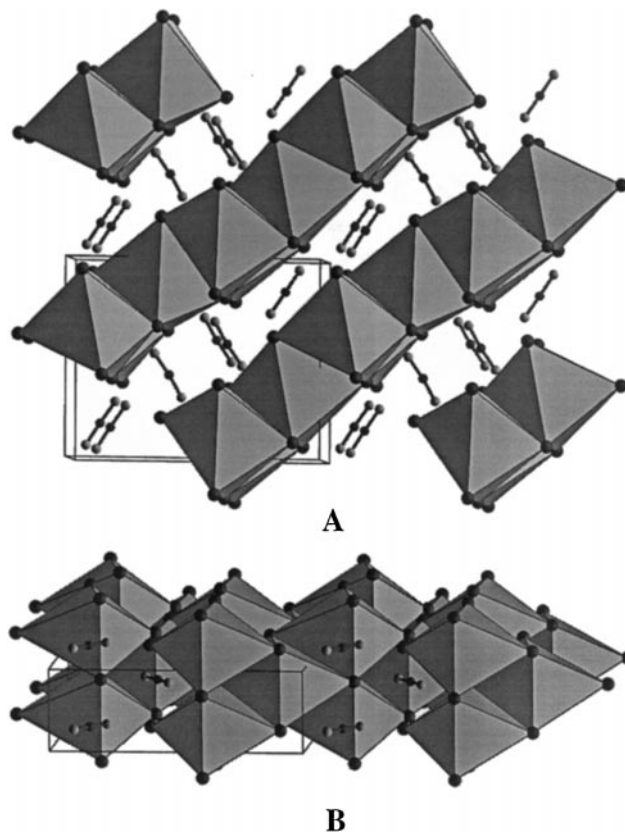


**FIG. 2.** Structure of Sr<sub>2</sub>BN<sub>2</sub>I: skew view along the *b*-axis [10]. The strontium atoms form octahedra around I<sup>-</sup>. The BN<sub>2</sub><sup>-</sup> units show pronounced deviations from linearity.

different compounds such as alkali metal suboxides (Cs<sub>11</sub>O<sub>3</sub>, [8]).

Comparing the local coordinations of the four strontium positions, the only differences to be found are the spatial

**TABLE 2**  
Atomic Coordinates and Equivalent Anisotropic Displacement Parameters (Å<sup>2</sup> × 10<sup>3</sup>) for Sr<sub>2</sub>BN<sub>2</sub>I

Atom	Site	<i>x</i>	<i>y</i>	<i>z</i>	<i>U</i> <sub>11</sub>	<i>U</i> <sub>22</sub>	<i>U</i> <sub>33</sub>	<i>U</i> <sub>12</sub>	<i>U</i> <sub>13</sub>	<i>U</i> <sub>23</sub>	<i>U</i> <sub>eq</sub>
Sr1	2e	0.0769(1)	1/4	0.9034(1)	13(1)	13(1)	13(1)	0	2(1)	0	13(1)
Sr2	2e	0.6496(1)	1/4	0.3695(1)	13(1)	12(1)	12(1)	0	-1(1)	0	12(1)
Sr3	2e	0.6034(1)	1/4	0.8271(1)	13(1)	13(1)	12(1)	0	-1(1)	0	12(1)
Sr4	2e	0.1934(1)	1/4	0.3842(1)	13(1)	12(1)	14(1)	0	1(1)	0	13(1)
I1	2e	0.0788(1)	1/4	0.6419(1)	14(1)	19(1)	18(1)	0	2(1)	0	17(1)
I2	2e	0.6530(1)	1/4	0.0959(1)	15(1)	19(1)	20(1)	0	3(1)	0	18(1)
N1	2e	0.4760(5)	1/4	0.6615(4)	11(2)	19(3)	13(2)	0	0(2)	0	14(1)
N2	2e	0.6958(5)	1/4	0.5550(4)	14(3)	19(3)	12(2)	0	1(2)	0	15(1)
N3	2e	0.2699(5)	1/4	0.2053(4)	18(3)	13(2)	13(2)	0	-2(2)	0	15(1)
N4	2e	0.0520(6)	1/4	0.0916(4)	16(3)	17(3)	16(2)	0	-4(2)	0	16(1)
B1	2e	0.5834(7)	1/4	0.6036(5)	15(3)	12(3)	10(3)	0	-5(2)	0	12(1)
B2	2e	0.1603(7)	1/4	0.1466(5)	16(3)	8(3)	9(3)	0	4(2)	0	11(1)

Note. *U*<sub>(eq)</sub> is defined as one-third of the trace of the orthogonalized *U*<sub>*ij*</sub> tensor. The components of the anisotropic displacement tensor take the form -2π<sup>2</sup> [h<sup>2</sup>*a*<sup>2</sup>*U*<sub>11</sub> + ... + 2*hka*\**b*\**U*<sub>12</sub>]. All the positions are fully occupied.

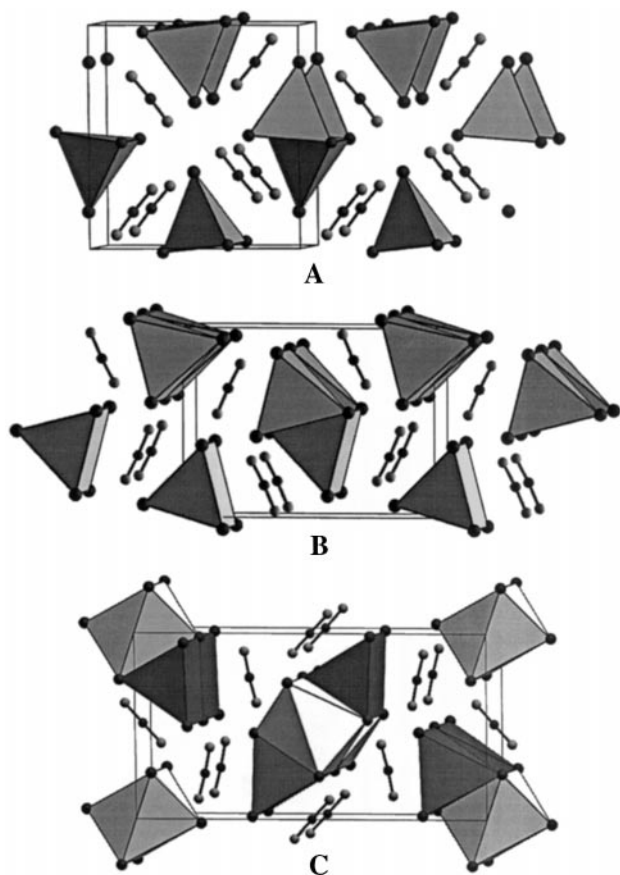


FIG. 3. (a) Structure of  $M_2BN_2F$  ( $M = Ca, Sr$ ; skew view along the  $b$ -axis): The alkaline-earth metal atoms form tetrahedra around  $F^-$  anions. (b) Structure of  $M_2BN_2Cl$  ( $M = Ca, Sr$ ; skew view along the  $b$ -axis): The alkaline-earth metal atoms form quadratic pyramids around  $Cl^-$  anions. (c) Structure of  $Eu_2BN_2Cl$  (skew view along the  $c$ -axis): The europium atoms form quadratic pyramids and octahedra around  $Cl^-$  anions.

distribution of the coordinated nitrido borate units. All the strontiums are surrounded by three iodides and three end-on coordinated  $BN_2^{3-}$  units according to the formulation  $[Sr(BN_2)_3I_3]$  (cf. Fig. 4). We assume a coordination to be end-on if the observed distances allow for a reasonable chemical interaction only with one of the terminal atoms of the  $BN_2$  group.

#### Geometry of $BN_2^{3-}$ Anions

The cumulated double bonds in the 16e systems impose a strong linear component onto the conformation of such units. Still, packing requirements and cation-anion interactions induce some distortion which may be taken to be significant. The B-N distances in  $Sr_2BN_2I$  vary between 132.2 and 135.4 pm. The angles ( $NBN = 174.4^\circ$  and  $178.6^\circ$ )

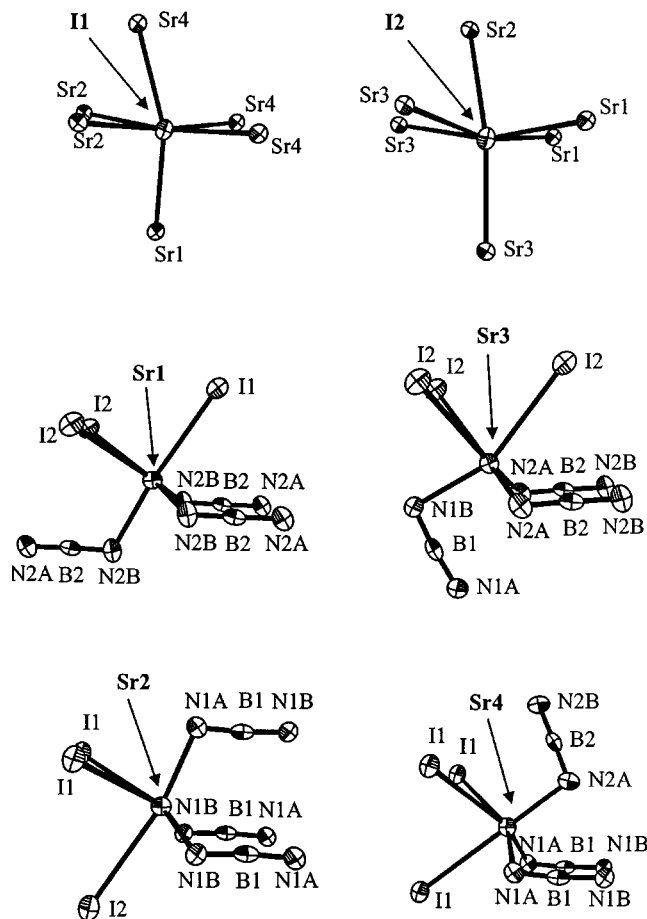


FIG. 4. Local coordinations in  $Sr_2BN_2I$  (90% probability ellipsoids [11]).

are, compared to other novel  $BN_2^{3-}$ -containing phases, quite small [5, 6]. See Tables 3 and 4.

#### Lattice Energy Calculation

$BN_2^{3-}$ -containing compounds can be understood as typical ionic compounds. The lattice energy, Madelung factors, and point potentials were calculated using the program MADKUG [9] which utilizes an Ewald procedure (Table 5). For the calculation of the Madelung factors a reference distance of 2.5 Å was used. The calculation of the Madelung parts of lattice energy (MAPLE) under assumption of the formal charges shows that the energy per unit charge is fairly high compared to rocksalt. The differences in the point potentials for all nitrogen in the two independent  $BN_2^{3-}$  units show a small polarization. The point potentials of N1B and N2B are higher than those of N1A and N2A. As in the fluoride and chloride compounds  $M_2BN_2X$  and  $M = Ca, Sr$  and  $X = F, Cl$  [6] the formally highly charged nitrido borate anions lie on the positions with the weakest point potential. This shows quite clearly that the halogenide

TABLE 3  
Bond Lengths [pm] for Sr<sub>2</sub>BN<sub>2</sub>I

Atom–Pair	<i>d</i>	<i>n</i>	Atom–Pair	<i>d</i>	<i>n</i>
Sr1–N2B	249.5(3)	2	Sr2–N1A	249.5(5)	
–N2B	251.0(5)		–N1B	250.7(3)	2
–B2	328.6(5)	2	–B1	318.4(7)	
–B2	332.2(7)		–B1	321.8(6)	2
–I1	346.45(7)		–I1	350.69(6)	2
–I2	348.98(6)	2	–I2	362.50(7)	
Sr3–N2A	252.2(3)	2	Sr4–N2A	250.8(5)	
–N1B	253.7(5)		–N1A	252.6(3)	2
–B1	296.5(7)		–B1	312.1(5)	2
–B2	323.4(5)	2	–B2	316.1(7)	
–I2	354.04(6)	2	–I1	351.95(6)	2
–I2	359.09(7)		–I1	362.78(7)	
I1–Sr1	346.45(7)		I2–Sr1	348.98(6)	2
–Sr2	350.69(6)	2	–Sr3	354.04(6)	2
–Sr4	351.95(6)	2	–Sr3	359.09(7)	
–Sr4	362.78(7)		–Sr2	362.50(7)	
N1B–B1	135.4(9)		N1A–B1	135.4(9)	
–Sr2	250.7(3)	2	–Sr2	249.5(5)	
–Sr3	253.7(5)		–Sr4	252.6(3)	2
N2A–B2	135.4(9)		N2B–B2	132.2(9)	
–Sr4	250.8(5)		–Sr1	249.5(3)	2
–Sr3	252.2(3)	2	–Sr1	251.0(5)	
B1–N1A	133.1(9)		B2–N2B	132.2(9)	
–N1B	135.4(9)		–N2A	136.0(9)	
–Sr3	296.5(7)		–Sr4	316.1(7)	
–Sr4	312.1(5)	2	–Sr3	323.4(5)	2
–Sr2	318.4(7)		–Sr1	328.6(5)	2
–Sr2	321.8(6)	2	–Sr1	332.2(7)	

part of the structure plays a prominent role in terms of coulombic energy. Of course, all other interactions are neglected in this approach.

TABLE 4  
Angles [°] for Sr<sub>2</sub>BN<sub>2</sub>I

N2–B1–N1	174.4(7)	N4–B2–N3	178.6(7)
----------	----------	----------	----------

TABLE 5  
Results of Lattice Energy Calculation for Sr<sub>2</sub>BN<sub>2</sub>I [9]: Madelung Factor, Lattice Energy (kJ C<sup>-2</sup> mol<sup>-1</sup>), Electrostatic Point Potentials *P* [a.u.], First Coordination Numbers (CN), and Mean Coordination Distances  $\bar{d}$  [pm]

Atom	<i>P</i>	CN/ $\bar{d}$	Atom	<i>P</i>	CN/ $\bar{d}$
Sr1	– 1.082	6/299.1	N1B	0.314	4/222.6
Sr2	– 1.128	6/302.5	N1A	0.343	4/221.4
Sr3	– 1.157	6/304.2	N2A	0.298	4/222.7
Sr4	– 1.164	6/320.5	N2B	0.363	4/220.6
I1	0.611	6/352.4	B1	– 0.155	2/134.3
I2	0.603	6/354.6	B2	– 0.127	2/134.1
<i>M<sub>F</sub></i>	17.01		MAPLE	383.9	

Note. Formal charges according to Sr<sup>2+</sup>, I<sup>–</sup>, N<sup>–</sup>, B<sup>–</sup> have been applied.

#### ACKNOWLEDGMENT

This work was supported by the Swiss National Science Foundation under Project 20-43-228.95.

#### REFERENCES

1. J. Goubeau and W. Anselmet, *Z. Anorg. Allg. Chem.* **310**, 248 (1961).
2. T. Sato, T. Endo, S. Kashima, O. Fukunaga, and M. Iwata, *J. Mater. Sci.* **18**, 3054 (1983).
3. P. Pyykkö, *J. Phys. Chem.* **94**, 7753 (1990).
4. M. Somer, U. Herterich, J. Curda, W. Carrillo-Cabrera, A. Zürn, K. Peters, and H. G. von Schnering, *Z. Anorg. Allg. Chem.*, in press.
5. F. E. Rohrer, Dissertation Eidgenössische Technische Hochschule, Zürich, 1997.
6. F. E. Rohrer and R. Nesper, *J. Solid State Chem.* **135**, 194 (1998).
7. G. M. Sheldrick, SHELXL93, A Program for the Refinement of Crystal Structures, Univ. Göttingen 1993.
8. A. Simon and E. Westerbeck, *Z. Anorg. Allg. Chem.* **428**, 187 (1977).
9. R. Nesper, G. Roch, W. Neukäter, and H. G. von Schnering, MAD-KUG, A Program for the Calculation of Lattice Energies, Madelung Factors, and Point Potentials, University of Münster, 1962; R. Nesper, updated versions, Max-Planck-Institut für Festkörperforschung Stuttgart 1984, Eidgenössische Technische Hochschule Zürich 1993.
10. P. Hofmann, COLTURE, Interactive Visualisation of Solid State Structures, Eidgenössische Technische Hochschule Zürich, 1995.
11. Siemens Analytical X-ray Systems, XP, "SHELXTL Version 5, Reference Manual," Madison, Wisconsin, 1996.